JACS
JOURNAL OF THE AMERICAN CHEMICAL SOCIETY
pubs.acs.org/JACS
Article

Covalent Degrader of the Oncogenic Transcription Factor β-Catenin

Flor A. Gowans,[#] Nafsika Forte,[#] Justin Hatcher, Oscar W. Huang, Yangzhi Wang, Belen E. Altamirano Poblano, Ingrid E. Wertz, and Daniel K. Nomura*

Cite This: J. Am. Chem. Soc. 2024, 146, 16856−16865
Read Online
ACCESS | Metrics & More | Article Recommendations | Supporting Information

ABSTRACT: β-catenin (CTNNB1) is an oncogenic transcription factor that is important in cell−cell adhesion and transcription of cell proliferation and survival genes that drive the pathogenesis of many different types of cancers. However, direct pharmacological targeting of CTNNB1 has remained challenging. Here, we have performed a screen with a library of cysteine-reactive covalent ligands to identify the monovalent degrader EN83 that depletes CTNNB1 in a ubiquitin-proteasome-dependent manner. We show that EN83 directly and covalently targets CTNNB1 three cysteines C466, C520, and C619, leading to destabilization and degradation of CTNNB1. Through structural optimization, we generate a highly potent and relatively selective destabilizing degrader that acts through the targeting of only C619 on CTNNB1. Our results show that chemoproteomic approaches can be used to covalently target and degrade challenging transcription factors like CTNNB1 through destabilization-mediated degradation.

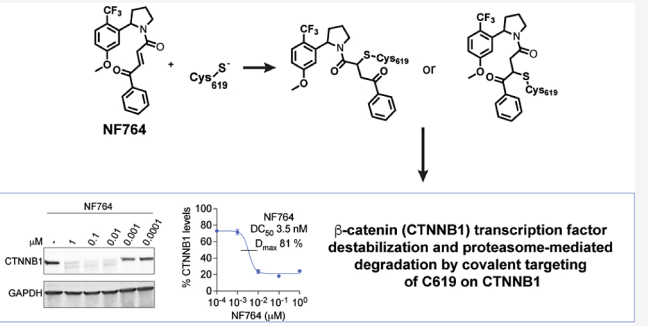

INTRODUCTION

β-catenin (CTNNB1) is an oncogenic transcription factor that drives the pathogenesis of many different types of human cancers, including liver, lung, colorectal, breast, and ovarian cancers.[1−3] CTNNB1 regulates cell−cell adhesion as part of a larger protein complex with E-cadherin and α-catenin. CTNNB1 is also a transcription factor that is activated by upstream Wnt signaling pathways that regulate genes involved in cell proliferation, survival, epithelial-to-mesenchymal transition, migration, and metastasis.[1−3] CTNNB1 is highly regulated by the ubiquitin-proteasome system, wherein the E3 ubiquitin ligase β-TrCP1 recognizes N-terminus of CTNNB1 upon phosphorylation by GSK3α and GSK3β.[1−3] Mutations in CTNNB1 are commonly found in a variety of cancers that are often located in the N-terminal segment that is recognized by E3 ligases, preventing ubiquitination and degradation of CTNNB1, thereby enhancing CTNNB1 oncogenic transcriptional activity.[1−3] Mutations have also been found in the Wnt pathway, including in APC and axin that act to enhance CTNNB1 levels and activity.[1−3]

Many efforts have been made to target the Wnt pathway for cancer therapy.[4−8] PKF115-584 and CGP04090 disrupt interactions between CTNNB1 and TCF.[4,5] However, the mechanism of inhibition of these compounds is poorly understood, and these compounds contain functional groups like quinones or taxoflavins that are concerning substructures associated with pan assay interference compounds (PAINS).[5] ICG-001 disrupts binding between CTNNB1 and CBP through binding with CBP and are not particularly potent with micromolar potency.[6] Tankyrase inhibitors, such as IWR-1 and XAV939, stabilize axin and the CK1 activator pryivinium to enhance the activity of the destruction complex, but these compounds do not directly interact with CTNNB1.[7,9] Also,while Wnt pathway inhibitors are promising, there are many mutations in the Wnt pathway found in many human tumors that may render these indirectly acting compounds ineffective.[1] Directly acting inhibitors or degraders of CTNNB1 would be preferable as a potential cancer therapeutic, but direct targeting of oncogenic transcription factors like CTNNB1 has also remained challenging due to its structural flexibility, intrinsic disorder, and lack of ligandable hotspots.[2] Direct CTNNB1 binding degraders such as methyl 3-{[(4-methylphenyl)sulfonyl]amino}benzoate) or MSAB that attenuate colorectal tumor growth have also been discovered, but the selectivity of these compounds and whether they exert their action on CTNNB1 through direct or indirect mechanisms are not clear.[8] Based on an axin-derived peptide that binds to CTNNB1, previous studies have also generated PROTACs that degrade CTNNB1, but the degradative selectivity of these compounds is unknown, and the potency of CTNNB1 degradation was in the high micromolar range.[10] Given the rapid turnover rate of CTNNB1, more durable pharmacological

Received: April 15, 2024
Revised: May 28, 2024
Accepted: May 29, 2024
Published: June 6, 2024

https://doi.org/10.1021/jacs.4c05174
J. Am. Chem. Soc. 2024, 146, 16856−16865

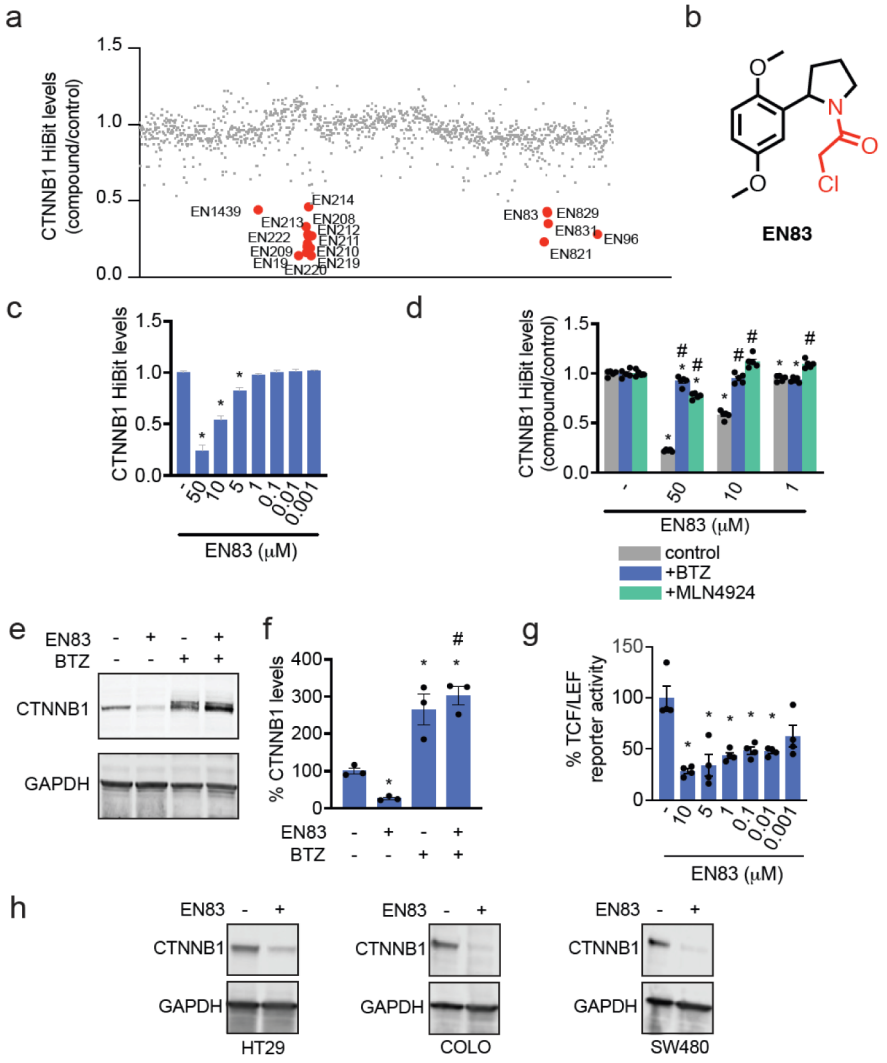

Figure 1. Covalent ligand screening to identify covalent CTNNB1 degraders. (a) Covalent ligand screen to identify compounds that lower CTNNB1 levels in cells. HEK293 cells expressing a N-terminal HiBiT-tagged CTNNB1 in the endogenous CTNNB1 locus were treated with DMSO vehicle or a cysteine-reactive covalent ligand (50 μM) for 24 h, and HiBiT-CTNNB1 levels were quantified. Data is shown as ratio of compound treatment/DMSO. Shown in red are compounds where there was >50% reduction in HiBiT-CTNNB1 levels. Primary screening data and structures of compounds screened can be found in Table S1. (b) Structure of main hit EN83 that showed reproducible lowering of HiBiT-CTNNB1 levels where the loss of CTNNB1 was attenuated by a proteasome inhibitor. (c) Dose-responsive lowering of HiBiT-CTNNB1 levels with EN83 treatment. HiBiT-CTNNB1 HEK293 cells were treated with DMSO vehicle or EN83 for 24 h. (d) Attenuation of EN83-mediated lowering of HiBiT-CTNNB1 levels upon proteasome and NEDDylation inhibitor pretreatment. HiBiT-CTNNB1 HEK293 cells were pretreated with DMSO vehicle, proteasome inhibitor bortezomib (1 μM), or NEDDylation inhibitor MLN4924 (1 μM) for 1 h prior to treatment of cells with DMSO vehicle or EN83 for 24 h. (e) EN83-mediated lowering of CTNNB1 protein levels is attenuated by proteasome inhibitor. Conditions of treatment were as described in (d) but CTNNB1 and loading control GAPDH levels were assessed by Western blotting. (f) Quantification of experiment from (e). (g) TCF/LEF luciferase reporter activity of WNT/CTNNB1 transcriptional activity in HEK293 cells. HEK293 cells were transfected with the TCF/LEF luciferase reporter construct and then treated with DMSO vehicle or EN83 for 24 h after which luciferase activity was quantified. (h) CTNNB1 levels in colorectal cancer cells. HT29, COLO, and SW480 colorectal cancer cells were treated with DMSO vehicle or EN83 (50 μM) for 2 h. Cells that had lost adherence but were still viable were collected, and CTNNB1 and loading control GAPDH levels were assessed by Western blotting. Blots and data in (c–h) are from $n = 3–6$ biologically independent replicates/group, where blots are representative from the replicates. Bar graphs in (c, d, f, g) show average ± sem values, and bar graphs in (d, f, g) also show individual replicate values. Significance (c, d, f, g) shown as $*p < 0.05$ compared to DMSO-treated controls and $\#p < 0.05$ compared to EN83 treatment alone for each concentration group.

strategies are needed to directly and fully target, degrade, and inhibit the activity of CTNNB1 for cancer therapy.[8]

There has been a recent surge in covalent drug discovery because of the ability of covalent drugs to access classically undruggable targets as well as shallower binding pockets through a combination of reactivity and affinity-driven mechanisms.[11] With advances in covalent chemoproteomic strategies such as activity-based protein profiling (ABPP), the overall target engagement and proteome-wide selectivity of these compounds can also be assessed and coupled with medicinal chemistry efforts to not only optimize potency but also specificity to eventually reduce off-target toxicological liabilities.[12−15] Covalent chemistry may also enable unique access to rare but kinetically accessible states of proteins that may be highly dynamic or intrinsically disordered such as many intractable transcription factors. Consistent with this premise, we have discovered covalent ligands that target intrinsically disordered cysteines within E3 ubiquitin ligases and deubiquitinases that

https://doi.org/10.1021/jacs.4c05174
J. Am. Chem. Soc. 2024, 146, 16856−16865

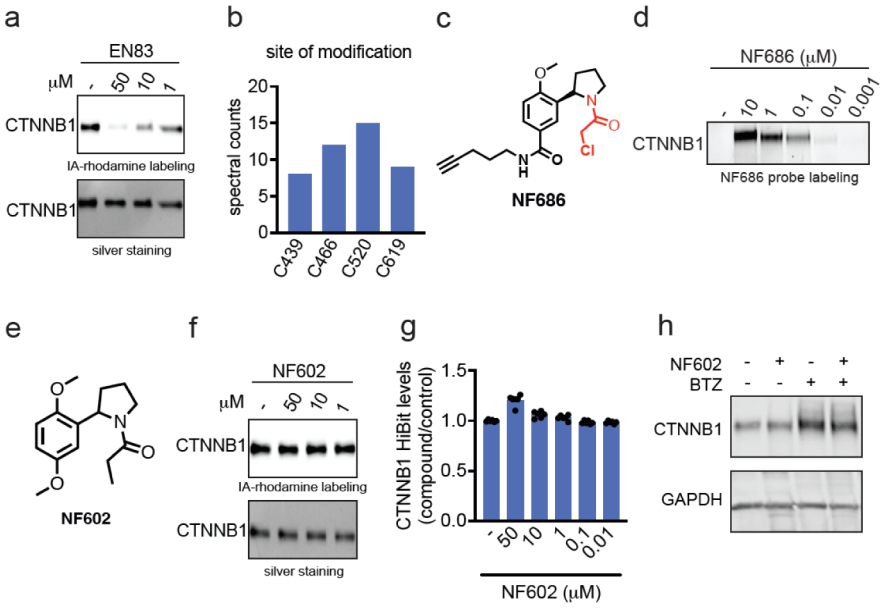

Figure 2. EN83 directly engages CTNNB1. (a) Gel-based ABPP analysis of EN83. Pure human CTNNB1 protein was preincubated with DMSO vehicle or EN83 for 30 min prior to labeling with a rhodamine-functionalized cysteine-reactive iodoacetamide probe (IA-rhodamine) (100 nM) for 60 min after which proteins were separated on SDS/PAGE, and IA-rhodamine labeling was assessed by in-gel fluorescence, and protein loading was assessed by silver staining. (b) MS/MS analysis of EN83 site of modification on CTNNB1. Pure CTNNB1 protein was incubated with EN83 (50 μM) for 30 min after which the protein was digested with trypsin and analyzed by LC−MS/MS to look for EN83-modified cysteines. Annotated are spectral counts for four cysteines on CTNNB1 that had EN83 modifications. (c) Structure of alkyne-functionalized analogue of EN83, NF686. (d) NF686 direct covalent labeling of CTNNB1. Pure human CTNNB1 protein was labeled with DMSO vehicle or NF686 for 1 h. Probe-labeled proteins were subjected to copper-catalyzed azide−alkyne cycloaddition (CuAAC) with rhodamine-azide after which proteins were separated by SDS/PAGE, and probe labeling was assessed by in-gel fluorescence. (e) Structure of nonreactive analogue of EN83, NF602. (f) Gel-based ABPP of NF602 performed as described in (a). (g) CTNNB1 levels with NF602 treatment. HiBiT-CTNNB1 HEK293 cells were treated with DMSO vehicle or NF602 for 24 h. (h) CTNNB1 protein levels with NF602 treatment. CTNNB1 HEK293 cells were treated with DMSO vehicle or NF602 for 24 h, and CTNNB1 and loading control GAPDH levels were assessed by Western blotting. Data in (a, b, d, f, g, h) are from $n = 3$−6 biologically independent replicates/group. Gels or blots shown in (a, d, f, h) are representative of the replicates. Data shown in (g) is shown as average ± sem values with individual replicates shown.

could be exploited for targeted protein degradation or stabilization applications.[16,17] We also previously discovered a covalent ligand EN4 that targeted an intrinsically disordered cysteine within MYC to inhibit MYC transcriptional activity and destabilize and degrade MYC, leading to antitumorigenic effects.[18] A recent study by Cravatt, Erb, et al. also demonstrated covalent targeting of a cysteine within the pioneer transcription factor FOXA1, resulting in rewiring of its transcriptional specificity and activity.[19] The Bar-Peled group recently covalently targeted a cysteine within the melanoma-driving transcription factor SOX10.[20] Collectively, these studies have suggested that covalent ligands may uniquely enable targeting of classically intractable oncogenic transcription factors, such as CTNNB1.

In this study, we screened a cysteine-reactive covalent ligand library to discover an early stage covalent monovalent degrader of CTNNB1 that acted through the direct targeting of cysteines on CTNNB1. We further optimized our initial hit compound to yield a highly potent covalent degrader of CTNNB1 that acts through a destabilization-mediated proteasome-dependent degradation mechanism, revealing a unique ligandable cysteine within a disordered region of CTNNB1 that can be targeted to inhibit CTNNB1 function.

RESULTS

Discovery of a Covalent Degrader of CTNNB1. To identify a covalent degrader of CTNNB1, we screened a library of 2100 cysteine-reactive covalent ligands consisting of acrylamides and chloroacetamides in HEK293 cells, expressing CTNNB1 with a N-terminal HiBiT tag incorporated into the endogenous loci of CTNNB1 (Figure 1a, Table S1). We identified 17 hits that decreased CTNNB1 levels. We subsequently eliminated hits that had appeared in previous screens conducted in our lab and counterscreened seven resulting hits to identify compounds that showed attenuation in CTNNB1 loss upon preincubation with either a proteasome inhibitor bortezomib or the Cullin E3 ligase NEDDylation inhibitor MLN4924 (Figure S1). We identified EN83 as the only hit that showed dose-responsive CTNNB1 loss that was significantly attenuated by proteasome or NEDDylation inhibition, indicating that EN83 was acting as a CTNNB1 degrader through a ubiquitin-proteasome-mediated mechanism (Figure 1b−d; Figure S1). We further confirmed the proteasome-mediated loss of CTNNB1 by Western blotting in HEK293T cells (Figure 1e,f). CTNNB1 transcriptional activity was significantly inhibited in a dose-dependent manner by EN83, demonstrating functional inhibition of the WNT pathway in cells (Figure 1g). We observed higher potency against CTNNB1 transcriptional activity in cells compared to CTNNB1 degradation, suggesting that EN83 may be engaging CTNNB1 at lower concentrations to inhibit CTNNB1 activity, while degradation of CTNNB1 requires higher engagement or concentrations. While CTNNB1 mRNA levels were unchanged, EN83 treatment significantly reduced the levels of CTNNB1 target gene MYC (Figure S2a). We also demonstrated the loss of

https://doi.org/10.1021/jacs.4c05174
J. Am. Chem. Soc. 2024, 146, 16856−16865

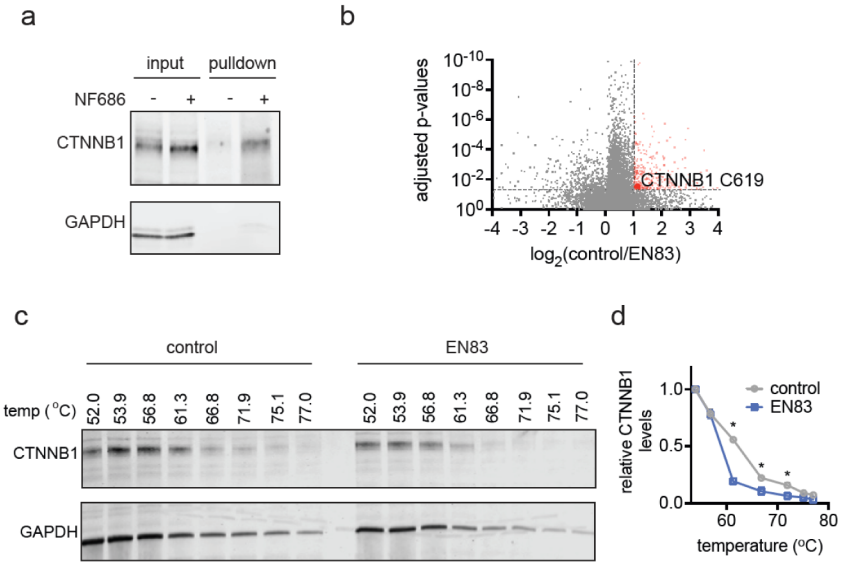

Figure 3. Characterization of EN83 interactions with CTNNB1 in cells. (a) NF686 enrichment of CTNNB1 from cells. HiBiT-CTNNB1 HEK293 cells were treated with DMSO vehicle or NF686 (50 μM) for 24 h, after which lysates were subjected to CuAAC with biotin-azide, and probe-labeled proteins were avidin-enriched, eluted, and CTNNB1 and unrelated protein GAPDH input and pulldown levels were detected by Western blotting. (b) Cysteine chemoproteomic profiling of EN83 by isoDTB-ABPP. HiBiT-CTNNB1 HEK293 cells were treated with DMSO vehicle or EN83 (10 μM) for 2 h. Lysates were then labeled with an alkyne-functionalized iodoacetamide probe (IA-alkyne) (200 μM) for 1 h, followed by appendage of isotopically light or heavy desthiobiotin-azide handles by CuAAC, after which probe-modified proteins were avidin-enriched, tryptically digested, and probe-modified peptides were eluted and analyzed by LC−MS/MS, and control versus treated or light versus heavy probe-modified peptide ratios were quantified. Shown in red are probe-modified peptides that showed a ratio greater than 2 with adjusted p-values less than 0.05 with C619 of CTNNB1 shown as significantly engaged. Chemoproteomics data can be found in Table S2. (c) Cellular thermal shift assay with EN83 treatment. HiBiT-CTNNB1 HEK293 cells were treated with DMSO or EN83 (50 μM) for 1 h after which cells were heated to the designated temperatures, insoluble proteins were precipitated, and CTNNB1 and GAPDH were detected by Western blotting. (d) Quantification of experiment in (c). Blots in (a, c) are representative of and quantitation of data in n = 3 biologically independent replicates/group. Chemoproteomic data in (b) and quantified data in (d) are from n = 3 biologically independent replicates/group. Data shown in (d) is shown as average ± sem values. Significance in (d) shown as *p < 0.05 compared to DMSO-treated controls for each temperature.

CTNNB1 in colorectal cancer cells that are driven by CTNNB1, including HT29, COLO, and SW480 cancer cell lines (Figure 1h). EN83 was also not acutely toxic to HT29 colorectal cancer cells (Figure S2b). We note that while we observed CTNNB1 loss in the HiBiT-tagged CTNNB1-expressing HEK293T cells at 24 h, we only observed CTNNB1 loss in HT29, COLO, and SW480 cells at earlier acute time points of 2 and 4 h, but CTNNB1 levels had recovered by 24 h in these cancer cell lines. This may be due to more rapid turnover rates of CTNNB1 in more cancer-relevant cell lines.

Characterization of EN83 as a Direct CTNNB1 Binder. We next sought to determine whether EN83 directly and covalently binds to CTNNB1. We found that EN83 dose-responsively displaced cysteine-reactive fluorescent probe labeling of pure human CTNNB1 protein by gel-based ABPP, indicating that EN83 directly engaged CTNNB1 pure protein through targeting cysteine(s) on CTNNB1 (Figure 2a). We further performed tandem mass spectrometry analysis (MS/MS) on tryptic digests from CTNNB1 pure protein incubated with EN83 and found four cysteines that were modified by EN83—C439, C466, C520, and C619 (Figure 2b). Interestingly, each of these cysteines resides in armadillo repeat motifs within the CTNNB1 structure, suggesting that these ligands may be binding across several structurally similar domains. To further confirm direct covalent binding of EN83 to CTNNB1, we synthesized an alkyne-functionalized analogue of EN83, NF686 and showed direct covalent dose-responsive probe labeling of pure CTNNB1 protein by NF686 (Figure 2c,d). We further demonstrated that the covalency is necessary since a nonreactive analogue of EN83, NF602, does not show binding to CTNNB1 and does not alter CTNNB1 levels by HiBiT or Western blotting detection (Figure 2e−h). Our results demonstrated that EN83 directly binds to CTNNB1.

We next wanted to confirm that EN83 engages with CTNNB1 in cells. We first used the alkyne probe NF686 in cells to demonstrate that CTNNB1 could be enriched from cells with the probe without enriching unrelated targets such as GAPDH (Figure 3a). We performed a mass spectrometry-based ABPP or isotopic desthiobiotin-ABPP (isoDTB-ABPP) to map the overall proteome-wide cysteine-reactivity of EN83 in cells using previously established methods.[13,16,21,22] These results showed that EN83 engaged C619 by >50% with statistical significance (adjusted p-value <0.05) (Figure 3b, Table S2). We did not detect the other three cysteines engaged by EN83 in our isoDTB-ABPP experiment, perhaps because these cysteines are not targeted by the iodoacetamide reactivity-based probe, or these peptides may not ionize well by MS-based methods from complex proteomes. As such, we cannot determine engagement of these other three cysteines, but our data shows significant engagement of C619 in CTNNB1. However, cysteine chemoproteomic profiling also revealed many other targets that were significantly engaged by EN83—308 other targets that were significantly engaged by >50% among 8251 cysteines detected and quantified across three biological replicates (Figure 3b, Table S2). Among the off-targets of EN83, none of the targets were within the Wnt signaling pathway, including AXIN1, BTRC, or GSK3A or GSK3B. While EN83 was not selective for CTNNB1, we were still intrigued by whether EN83 through

https://doi.org/10.1021/jacs.4c05174
J. Am. Chem. Soc. 2024, 146, 16856−16865

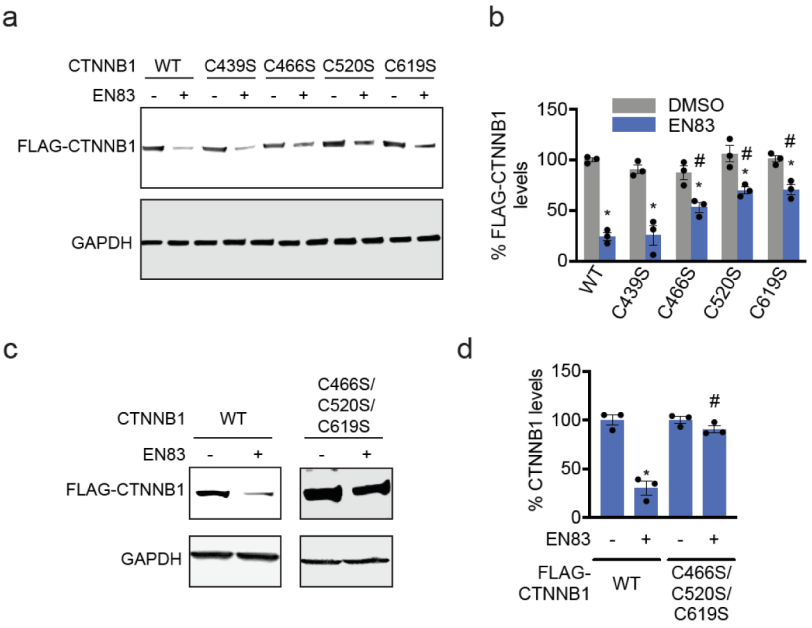

Figure 4. Cysteine mutant rescue of EN83-mediated CTNNB1 degradation. (a) HEK293T cells were transfected with FLAG-tagged wild-type (WT) or C439S, C466S, C520S, or C619S FLAG-tagged CTNNB1 mutants and treated with DMSO vehicle or EN83 (10 μM) for 24 h, after which FLAG and loading control GAPDH were detected by Western blotting. (b) Quantification of experiment from (a).(c) HEK293T cells were transfected with FLAG-tagged wild-type (WT) or C466S/C520S/C619S FLAG-tagged CTNNB1 triple mutants and treated with DMSO vehicle or EN83 (10 μM) for 24 h, after which FLAG and loading control GAPDH were detected by Western blotting. (d) Quantification of experiment from (c). Blots from (a, c) are representative of $n = 3$ biologically independent replicates/group and individual replicate values and average ± sem are shown in corresponding bar graphs in (b, d). Significance in (b, d) expressed as $^*p < 0.05$ compared to each respective DMSO-treated control group and $\#p < 0.05$ compared to the EN83-treated wild-type FLAG-CTNNB1 control group.

direct covalent targeting of CTNNB1 was leading to its degradation and considered this compound as a "pathfinder probe"[23] to identify approaches to CTNNB1 ligandability that could be later optimized through medicinal chemistry efforts. Cellular thermal shift assay from EN83 cellular treatment showed significant thermal destabilization of CTNNB1 in the cells. These results further demonstrated that EN83 directly engages CTNNB1 and also suggested that the degradation of CTNNB1 may be caused by direct covalent targeting of CTNNB1, leading to destabilization of CTNNB1 folding and subsequent ubiquitination and degradation (Figure 3c,d).

We next sought to confirm whether the cysteines targeted by EN83 in CTNNB1 were contributing to its degradation. We expressed either FLAG-tagged wild-type, C439S, C466S, C520S, or C619S mutant CTNNB1 in cells and showed that mutation of C466, C520, or C619, but not C439, to serines significantly attenuated CTNNB1 degradation in cells (Figure 4a,b). Consistent with the role of these three cysteines in CTNNB1 degradation, mutation of C466, C520, and C619 to serines led to the complete attenuation of FLAG-CTNNB1 loss (Figure 4c,d). These results demonstrated that direct targeting of three out of the four cysteines identified within CTNNB1 led to the degradation of CTNNB1 and that the loss of CTNNB1 was not through an indirect mechanism or through one of the many off-targets of EN83.

Improving Potency and Selectivity of EN83 against CTNNB1. Toward improving potency of EN83 against CTNNB1 and exploring structure−activity relationships, we synthesized several analogues of EN83. EN83 is a racemic mixture of two enantiomers. We first separated the individual enantiomers by chiral chromatography to determine whether there was a particular enantiomer that was more potent. Both enantiomers of EN83 showed comparable lowering of CTNNB1 levels by HiBiT and proteasome-mediated CTNNB1 degradation by Western blotting and showed equivalent CTNNB1 binding, indicating that there was no difference between the two enantiomers (Figure S2c−e). We also sought to replace the chloroacetamide cysteine-reactive warhead, which may possess metabolic liabilities for further development. Replacement with an acrylamide warhead (NF601) found in many orally bioavailable covalent drugs, such as the BTK inhibitor ibrutinib or the KRAS G12C inhibitor sotorasib,[11] unfortunately compromised binding to CTNNB1 and did not show CTNNB1 loss in either HiBiT or Western blotting detection approaches (Figure S3a−d). We found that replacement of the methoxy groups with trifluoromethyl moieties, NF740 and NF741, was tolerated for both binding to CTNNB1 by gel-based ABPP and lowering CTNNB1 HiBiT levels in HEK293 cells in a dose-responsive manner (Figure S3e−g). This lowering of CTNNB1 was also confirmed to be proteasome dependent (Figure S3h). We found that replacement of the chloroacetamide warhead with an oxo-phenylbutenamide warhead with NF764 improved CTNNB1 binding (Figure 5a,b). Analysis of the NF764 site of modification on pure CTNNB1 protein revealed that only C619 but not C439, C466, or C520 was adducted by NF764 (Figures S4a, 5c). Cysteine chemoproteomic profiling of NF764 revealed significant engagement of CTNNB1 C619 with a ratio of 3.7, indicating 73% engagement at 10 nM in HT29 colorectal cancer cells. This profiling also revealed that NF764 was much more selective than EN83 with 61 significant off-targets of NF764 with ratio >3 among 7626 cysteines quantified (Figure 5d, Table S3). Strikingly, NF764 potently degraded CTNNB1 with a 50% degradation concentration (DC_{50}) of 3.5 nM with a $D_{max.}$ of 81%

https://doi.org/10.1021/jacs.4c05174
J. Am. Chem. Soc. 2024, 146, 16856−16865

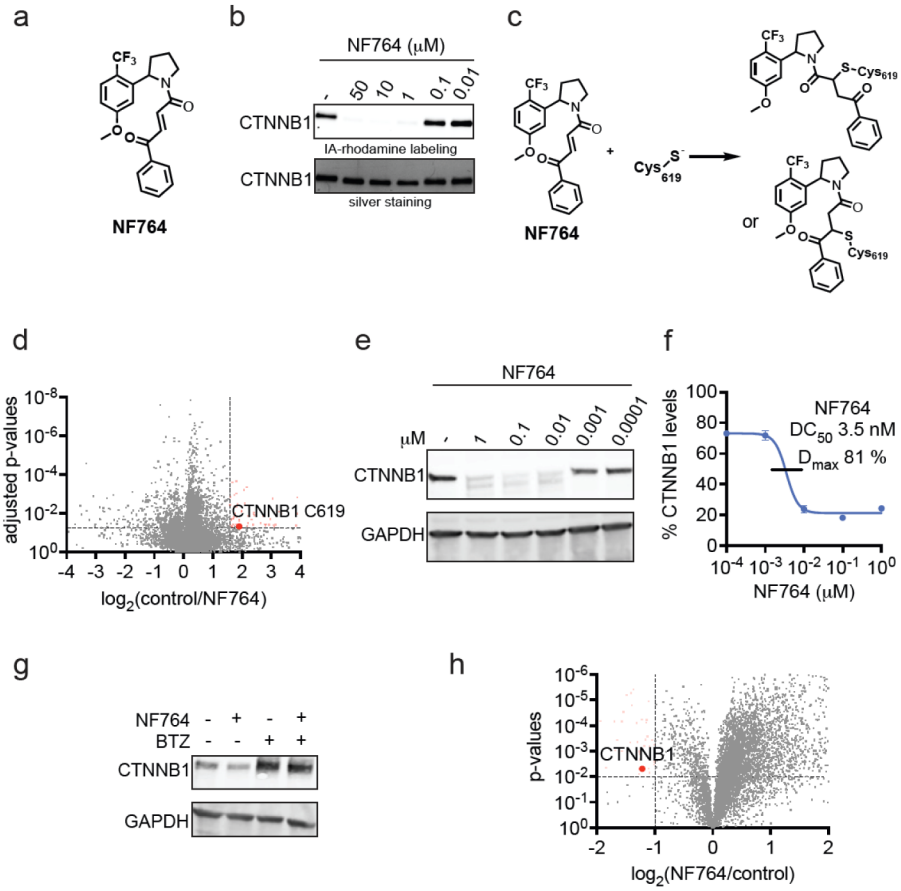

Figure 5. Characterization of optimized CTNNB1 degrader NF764. (a) Structures of optimized EN83 analogue NF764. (b) Gel-based ABPP analysis of NF764 against CTNNB1. CTNNB1 pure protein was preincubated with DMSO or NF764 30 min prior to IA-rhodamine labeling (100 nM) for 60 min, after which proteins were separated by SDS/PAGE, and probe labeling was assessed by in-gel fluorescence, and protein loading was assessed by silver staining. (c) Depiction of NF764 covalent adduct on C619 of CTNNB1 based on MS/MS analysis of NF764 site-of-modification in Figure S4. We do not yet know which of the two adducts are being formed on CTNNB1. (d) isoDTB-ABPP analysis of NF764 in HT29 cells. HT29 cells were treated with DMSO vehicle or NF764 (10 nM) for 2 h. Lysates were then labeled with an alkyne-functionalized iodoacetamide probe (IA-alkyne) (200 μM) for 1 h, followed by appendage of isotopically light or heavy desthiobiotin-azide handles by CuAAC, after which probe-modified proteins were avidin-enriched, tryptically digested, and probe-modified peptides were eluted and analyzed by LC−MS/MS, and control versus treated or light versus heavy probe-modified peptide ratios were quantified. Shown in red are probe-modified peptides that showed a ratio greater than 3 with adjusted p-values less than 0.05 with C619 of CTNNB1 shown as significantly engaged. Chemoproteomics data can be found in Table S3. (e) NF764-mediated CTNNB1 degradation in HT29 cells. HT29 cells were treated with DMSO vehicle of NF764 for 6 h. CTNNB1 and loading control GAPDH levels were assessed by Western blotting. (f) Quantification of experiment in (e) showing average ± sem values and DC_{50} of 3.5 nM and D_{max} of 81% for NF764. (g) Proteasome dependence of CTNNB1 loss. HiBiT-CTNNB1 HEK293 cells were pretreated with DMSO vehicle or bortezomib (1 μM) for 1 h prior to treatment with DMSO vehicle or NF764 (10 μM) for 24 h. CTNNB1 and loading control GAPDH levels were assessed by Western blotting. (h) TMT-based quantitative proteomic profiling of NF764 in HT29 cells. HT29 cells were treated with DMSO vehicle or NF764 (10 nM) for 4 h. Shown in red are proteins in which levels were reduced by NF764 treatment by >2-fold with $p < 0.05$. Highlighted is CTNNB1 as a significantly downregulated target. Gels and blots in (b, e, g) are representative of $n = 3$ biologically independent replicates/group. Chemoproteomic and proteomic experiments in (d, h) are from $n = 3$ biologically independent replicates/group and data are in Tables S3 and S4, respectively.

in HT29 cells (Figure 5e,f). This loss of CTNNB1 protein levels was still proteasome dependent (Figure 5g). Quantitative proteomic profiling of protein levels showed relatively selective loss of CTNNB1 with only 36 other proteins, changing significantly in levels alongside CTNNB1 with NF764 treatment by >2-fold among 6400 proteins quantified (Figure 5h; Table S4). Among these 37 other proteins, we noted that many proteins, including EFNB2, ITGB7, PCDH1, CDH17, CLDN4, CLDN7, LAMA3, LEO1, HMGCS2, ERN1, FABP1, and SLC7A5 are involved in cell−cell adhesion and cell−cell communication that is regulated by CTNNB1 or proteins that are known to be directly regulated by CTNNB1 protein interactions or transcriptional function.[24−32] As such, while these changes may be due to the off-target effects of NF764, many of the changes in protein levels may be through on-target mechanisms. NF764, like EN83, was not acutely cytotoxic in HT29 cells (Figure S4b). We further showed significant downregulation in the mRNA levels of several CTNNB1-target genes, including MYC, S100A6, AXIN2, and CCND1 (Figure S4c). Thus, we demonstrated that NF764 is a more potent and selective CTNNB1 binder and degrader.

To further validate that NF764 degrades CTNNB1 through only targeting C619, compared to EN83 that acts through targeting three cysteines, we demonstrated that FLAG-CTNNB1 C619S mutation expressing HEK293T cells are completely resistant to NF764-mediated CTNNB1 loss compared to cells expressing FLAG-CTNNB1 wild-type protein and that the C466S/C520S/C619S triple mutant expressing

https://doi.org/10.1021/jacs.4c05174
J. Am. Chem. Soc. 2024, 146, 16856−16865

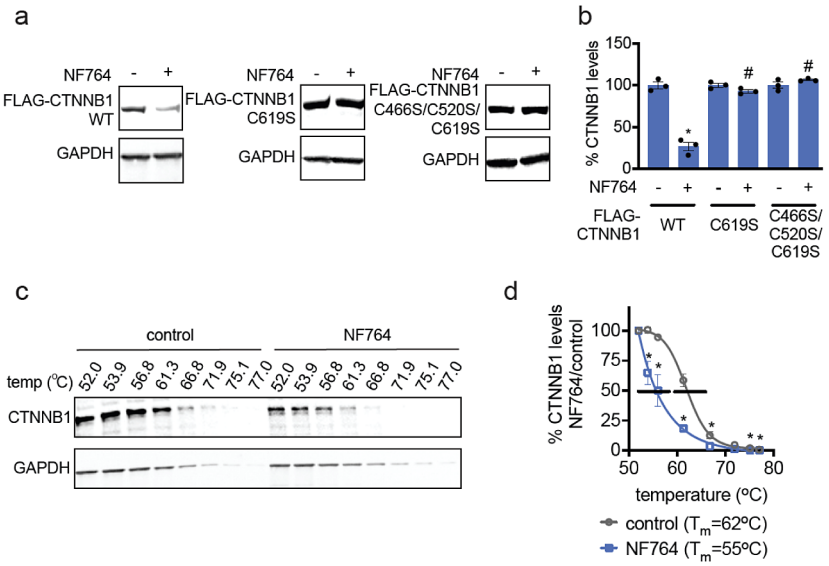

Figure 6. Cysteine mutant rescue of NF764-mediated CTNNB1 degradation. (a) HEK293T cells were transfected with FLAG-tagged wild-type (WT) or C619S or C466S/C520S/C619S FLAG-tagged CTNNB1 mutants and treated with DMSO vehicle or NF764 (5 μM) for 24 h, after which FLAG and loading control GAPDH were detected by Western blotting. (b) Quantification of experiment from (a). (c) Cellular thermal shift assay with NF764 treatment. HEK293 cells were treated with DMSO or NF764 (10 nM) for 1 h, after which cells were heated to the designated temperatures, insoluble proteins were precipitated, and CTNNB1 and GAPDH were detected by Western blotting. (d) Quantification of experiment from (c) with calculated 50% melting temperature (T_m) shown for CTNNB1. Blots from (a, c) are representative of $n = 3$ biologically independent replicates/group and individual replicate values and average ± sem are shown in corresponding bar graph in (b) and average ± sem values are shown in (d). Significance in (b, d) expressed as $*p < 0.05$ compared to each respective DMSO-treated control group and $\#p < 0.05$ compared to the NF764-treated wild-type FLAG-CTNNB1 group.

cells do not show any additional rescue beyond the single C619S mutation (Figure 6a,b). Cellular thermal shift analysis of NF764 also showed a more pronounced destabilization of CTNNB1 in HT29 cells, showing a 7 °C shift in melting temperature from 62 to 55 °C with NF764 treatment (Figure 6c,d). Thus, while our compound may still have off-targets, we demonstrate that the degradation of CTNNB1 by NF764 is mediated through direct covalent targeting of C619 on CTNNB1. We thus designate NF764 as a pathfinder compound that reveals a novel ligandable cysteine C619 that can be exploited for degradation of CTNNB1.

CONCLUSIONS

In this study, we identified a degrader of CTNNB1 that acts through direct covalent targeting of either C466, C520, or C619 or just C619 on CTNNB1 to destabilize and degrade CTNNB1 in a proteasome-dependent manner. We conjecture that the mode of degradation observed in this study is likely distinct from traditional modes of targeted protein degradation, such as proteolysis targeting chimeras (PROTACs) and molecular glue degraders and instead occurs through a thermodynamic destabilization of CTNNB1, resulting from direct covalent binding, leading to a destabilization-mediated degradation of CTNNB1.[33−35] Interestingly, C619 is predicted to be an intrinsically disordered cysteine within CTNNB1. We believe that this is analogous to our previous findings with another oncogenic transcription factor MYC, where we discovered a covalent ligand EN4 that irreversibly targeted another intrinsically disordered C171 in MYC, leading to a thermal destabilization and degradation of MYC.[18] Many transcription factors have often eluded classical drug discovery efforts because of their lack of well-defined binding pockets for small-molecule binding and because many of them possess large segments of unstructured or disordered regions. Whether through inhibition, activation, destabilization, or degradation, covalent ligands may be able to access dynamic and transient states or rare but kinetically accessible states of highly dynamic and intrinsically disordered proteins such as transcription factors to modulate their function in unique ways. A striking example of such functional modulation is a recent discovery by Erb, Cravatt, et al. of a covalent ligand that stereoselectively targeted a pioneer transcription factor FOXA1 to rewire its transcriptional programming.[19] Other examples of covalent ligand-assisted degradation include the TFIIH helicase ERCC3 and immune kinases such as ITK.[36,37] While challenging to prove, we conjecture that these intrinsically disordered regions within transcription factors may adopt a transient binding pocket that can be molecularly recognized by a covalent ligand to form an irreversible bond. Given that these disordered transcription factors may already be thermodynamically unstable, we hypothesize that it may not require significant binding energy to further destabilize these dynamic regions, leading to their unfolding and ultimately ubiquitination and degradation of these targets. It will be of future interest to demonstrate this type of transient molecular recognition of disordered regions within transcription factors with enantiomerically paired covalent ligands to garner stereoselective interactions with these sites.

While we demonstrate initial medicinal chemistry efforts to explore structure−activity relationships of EN83, leading to improved CTNNB1 binders and degraders, further medicinal chemistry efforts need to be performed to improve the potency, selectivity, and metabolic stability of the compounds reported here. We note that while we observed CTNNB1 loss at 24 h with EN83 treatment in the model cell line HEK293 cells, we only observed acute loss of CTNNB1 at 2 and 4 h with recovery by 24 h in more relevant colorectal cancer cell lines. CTNNB1 is heavily regulated by the ubiquitin-proteasome system and thus

https://doi.org/10.1021/jacs.4c05174
J. Am. Chem. Soc. 2024, 146, 16856−16865

may have faster turnover in cancer cell lines that are driven by CTNNB1[2]. As such, a covalent degrader of CTNNB1 would likely need to maintain target engagement and ultimately show sustained *in vivo* pharmacokinetics to achieve persistent pharmacodynamics. A covalent degrader that irreversibly engages CTNNB1 will show stoichiometric and noncatalytic degradation. A covalent reversible CTNNB1 degrader may be able to exploit the ligandable cysteines within CTNNB1, while achieving substoichiometric catalytic degradation of CTNNB1. Furthermore, we do not yet understand the mechanism of action of CTNNB1 degradation observed in this study. Follow-up studies using functional genomic screens to identify the E3 ligase(s) responsible for EN83 and NF764-mediated degradation would further enable the optimization of these degraders.

Nonetheless, compared to previously described CTNNB1 inhibitors that either act indirectly through targeting other components of the Wnt pathway or potentially act directly on CTNNB1 but modulate its function either nonpotently or with unknown mechanism or selectivity, we put forth a highly potent CTNNB1 degrader that acts through a unique mechanism of covalently targeting a novel ligandable C619 to destabilize and degrade CTNNB1. Overall, our study demonstrates the utility of using covalent chemoproteomic strategies to identify unique ligandable sites and covalent ligands that can directly target classically intractable target classes, such as transcription factors, to ultimately degrade targets such as CTNNB1 for potential future cancer therapy applications.

METHODS

Cell Culture. CTNNB1 HiBiT cells were commercially purchased from Promega (CS302340). HEK293, COLO-201, HT29, and SW480 were obtained from UC Berkeley's Biosciences Divisional Services Cell Culture Facility. HiBiT, HEK, and HT29 were cultured in DMEM, and COLO-201 cells were cultured in RPMI base media. Both media types contained 10% (v/v) fetal bovine serum (FBS), were supplemented with 1% glutamine, and were maintained at 37 °C with 5% CO_2.

Covalent Ligand Library and Synthesis of Other Compounds. Covalent ligands starting with "EN" are commercially available from Enamine LLC. Syntheses of other compounds are described in Supporting Information.

Covalent Ligand Screen with CTNNB1 HiBiT Cell Line. Covalent ligand screen and dose responses were conducted using a Promega Nano-Glo HiBiT Lytic Detection System (N3040) and CellTiter-Glo 2.0 Assay (G9242). HiBiT cells were seeded into 96-well plates (Corning 3917) at 35,000 cells per 100 μL of media and were left overnight to adhere. Cells were treated with 25 μL of media containing 1:125 dilution from a 1000× DMSO compound stock and treated for either 6, 12, or 24 h. The lytic detection system recipe was followed per Promega's suggestion. 125 μL of CTG or Lytic detection system reagents was added to each well. To assess the cells in the supernatant, half of the plates had the media removed prior to the addition of CTG or a lytic detection system reagents. Plates were rocked for 15 min prior to their luminescence readout on the Tecan Spark Plate reader (30086376).

Western Blotting. Pelleted cells are lysed with CST buffer containing protease inhibitor cocktail (Pierce A32955). Samples were centrifuged at 20,000*g* for 20 min at 4 °C to remove cell debris. Samples' protein content was normalized to run 30 μg per well. Samples were then boiled for 8 min at 90 °C after addition of 4× reducing Laemmli SDS sample loading buffer (Alfa Aesar) and ran on precast 4−20% Criterion TGX gels (Bio-Rad).

Antibodies to CTNNB1 (Cell Signaling Technology, 8814S), GAPDH (Proteintech Group Inc., 60004-1-Ig or Cell Signaling Technology, 14C10), and DDDDK tag (Abcam, ab205606) were diluted as per recommended manufacturers' procedures. Proteins were resolved by SDS/PAGE and transferred to nitrocellulose membranes using the BioRad system (1704271 and 1704150). Blots were blocked with 5% BSA in Tris-buffered saline containing Tween 20 (TBST) solution for 1 h at room temperature, washed in TBST, and probed with primary antibody diluted in recommended diluent per manufacturer overnight at 4 °C. Following washes with TBST, the blots were incubated in the dark with secondary antibodies purchased from Ly-Cor and used at 1:10,000 dilution in 5% BSA in TBST at room temperature. Blots were visualized using an Odyssey Li-Cor scanner after additional washes. If additional primary antibody incubations were required, the membrane was stripped using ReBlot Plus Strong Antibody Stripping Solution (EMD Millipore, 2504), washed, and blocked again before being reincubated with primary antibody.

β-Catenin Constructs. Human beta-catenin constructs (residues 151−661) were synthesized and inserted into a pET28a vector. For synthesis of the construct, a six-histidine tag next to a TEV protease site was placed on the n-terminal side of beta-catenin and a two-repeat linker of AEAAA followed by human TF7L2 18-49/avi on the c-terminal end of beta-catenin.

β-Catenin Purification. Beta-catenin constructs were expressed in *E. coli* DE3 pLys cells grown to OD of 600 at 37 °C and induced with 300 μM IPTG. Expression was allowed to proceed for 16 h at 16 °C. Cells were centrifuged at 5000*g* for 10 min then collected and frozen at −80 °C. *E. coli* cells were lysed three passes through a fluid homogenizer packed in ice. Cell debris was centrifuged at 103,000*g* for 30 min, and supernatant was added to 4 mL of Talon and allowed to batch bind for 6 0 min at 4 °C. Talon resin was washed with 50 CV of 50 mM TRIS pH 8.5, 500 mM NaCl, 10% glycerol, 0.5 mM TCEP, and 25 mM imidazole. Protein was eluted with 5 0 mM TRIS pH 8.5, 500 mM NaCl, 10% glycerol, 0.5 mM TCEP, and 300 mM imidazole until no protein could be visually detected by Coomassie blue protein assay. Eluted beta-catenin avi tagged protein was biotinylated with BirA enzyme overnight. Biotinylated protein was desalted to remove any free biotin then allowed to batch bind for 2 h to overnight to Streptavidin Mutein matrix. The protein was then eluted with 50 mM TRIS pH 8.5, 500 mM NaCl, 10% glycerol, 0.5 mM TCEP, and 2 mM biotin. Eluted protein was directly run over a S200 16/600 SEC column (50 mM TRIS pH 8.5, 500 mM NaCl, 10% glycerol, 0.5 mM TCEP).

Covalent Ligand Screen and Gel-Based ABPP with CTNNB1 Pure Protein. CTNNB1 pure protein (0.1 μg/25 μL in PBS) was treated with either DMSO vehicle or covalent ligand at 37 °C for 30 min and subsequently treated with 0.1 μM IA-rhodamine (Setareh Biotech) for 1 h at RT in the dark. The reaction was stopped by the addition of 4× reducing Laemmli SDS sample loading buffer (Alfa Aesar). After boiling at 95 °C for 5 min, the samples were separated on precast 4−20% Criterion TGX gels (Bio-Rad) and were analyzed by in-gel fluorescence using a ChemiDoc MP (Bio-Rad).

NF686 Probe Labeling on CTNNB1 NV03 Pure Protein. CTNNB1 pure protein (0.2 μg/50 μL in PBS) was treated with either DMSO vehicle or NF686 at 37 °C for 30 min. Click reagent Azide-Fluor 545 (Click Chemistry Tools, Inc. AZ109−

https://doi.org/10.1021/jacs.4c05174
J. Am. Chem. Soc. 2024, 146, 16856−16865

5), copper(II) sulfate, and TBTA (TCI Chemicals, T2993) were added to have a final concentration of 21.8 μM, 873.4 μM, and 47.2 μg/mL, respectively, for 1 h at RT in the dark. The reaction was stopped by addition of 4× reducing Laemmli SDS sample loading buffer (Alfa Aesar). After boiling samples at 95 °C for 5 min, the samples were separated on precast 4−20% Criterion TGX gels (Bio-Rad). Probe-labeled proteins were analyzed by in-gel fluorescence using a ChemiDoc MP instrument (Bio-Rad).

Luciferase Reporter Assay. HEK293 cells were seeded at a density of 30,000/well in 96-well white plate overnight. Each well was transiently cotransfected with 60 ng of TCF/LEF luciferase reporter vector and 60 ng of renilla luciferase control vector using Lipofectamine 2000, provided by TCF/LEF Reporter Kit Wnt/β-catenin signaling pathway (BPS Bioscience, #60500). After 72 h post-transfection, cells were then treated with EN83 or DMSO vehicle control until desired time point. Firefly and renilla luciferase reporter genes' expression levels were examined by TWO-Step Luciferase (Firefly and Renilla) Assay System (BPS Bioscience #60683) according to manufacturer's protocols. Luminescent signals were measured using the Tecan Spark Plate reader (30086376).

Chemoproteomic Profiling. Chemoproteomic profiling methods are described in the Supporting Information.

■ ASSOCIATED CONTENT

Supporting Information

The Supporting Information is available free of charge at https://pubs.acs.org/doi/10.1021/jacs.4c05174.

Figure S1, counterscreening data; Figure S2, characaterization of EN83; Figure S3, characterization of EN83 analogues; Figure S4, characterization of NF764; supporting methods, and synthetic methods and characterization (PDF)

Structures of compounds screened and screening data (Table S1) (XLSX)

Cysteine chemoproteomic profiling of EN83 (Table S2) (XLSX)

Cysteine chemoproteomic profiling of NF764 (Table S3) (XLSX)

Quantitative proteomic profiling of NF764 (Table S4) (XLSX)

■ AUTHOR INFORMATION

Corresponding Author

Daniel K. Nomura − *Department of Chemistry, University of California, Berkeley, California 94720, United States; Innovative Genomics Institute, Berkeley, California 94720, United States; Department of Molecular and Cell Biology, University of California, Berkeley, California 94720, United States;* orcid.org/0000-0003-1614-8360; Email: dnomura@berkeley.edu

Authors

Flor A. Gowans − *Department of Chemistry, University of California, Berkeley, California 94720, United States; Innovative Genomics Institute, Berkeley, California 94720, United States*

Nafsika Forte − *Department of Chemistry, University of California, Berkeley, California 94720, United States; Innovative Genomics Institute, Berkeley, California 94720, United States*

Justin Hatcher − *Department of Chemistry, University of California, Berkeley, California 94720, United States; Innovative Genomics Institute, Berkeley, California 94720, United States*

Oscar W. Huang − *Bristol Myers Squibb, San Francisco, California 94158, United States*

Yangzhi Wang − *Department of Chemistry, University of California, Berkeley, California 94720, United States; Innovative Genomics Institute, Berkeley, California 94720, United States;* orcid.org/0000-0002-4972-0960

Belen E. Altamirano Poblano − *Department of Chemistry, University of California, Berkeley, California 94720, United States; Innovative Genomics Institute, Berkeley, California 94720, United States*

Ingrid E. Wertz − *Bristol Myers Squibb, San Francisco, California 94158, United States*

Complete contact information is available at: https://pubs.acs.org/10.1021/jacs.4c05174

Author Contributions

#F.A.G. and N.F. contributed equally to this work

Notes

The authors declare the following competing financial interest(s): OWH was an employee of Bristol Myers Squibb when this study was initiated, but is now an employee of Lyterian Therapeutics. IEW was an employee of Bristol Myers Squibb when this study was initiated but is now a co-founder and the CEO of Lyterian Therapeutics. IEW is on the Scientific Advisory Boards of PAIVBio and Firefly Biologics. DKN is a co-founder, shareholder, and scientific advisory board member for Frontier Medicines and Vicinitas Therapeutics. DKN is a member of the board of directors for Vicinitas Therapeutics. DKN is also on the scientific advisory board of The Mark Foundation for Cancer Research, Photys Therapeutics, Apertor Pharmaceuticals, and Deciphera Pharmaceuticals. DKN is also an Investment Advisory Partner for a16z Bio, an Advisory Board member for Droia Ventures, and an iPartner for The Column Group.

■ ACKNOWLEDGMENTS

We thank the members of the Nomura Research Group and Bristol Myers Squibb for critical reading of the manuscript. This work was supported by Bristol Myers Squibb for all listed authors. This work was also supported by the Nomura Research Group and the Mark Foundation for Cancer Research ASPIRE Award for DKN. This work was also supported by grants from the National Institutes of Health (R01CA240981 and R35CA263814 for DKN). We also thank H. Celik and UC Berkeley's NMR facility in the College of Chemistry (CoC-NMR) for spectroscopic assistance. Instruments in the College of Chemistry NMR facility are supported in part by NIH S10OD024998.

■ REFERENCES

(1) Bugter, J. M.; Fenderico, N.; Maurice, M. M. Mutations and mechanisms of WNT pathway tumour suppressors in cancer. *Nat. Rev. Cancer* **2021**, *21*, 5−21.

(2) Anastas, J. N.; Moon, R. T. WNT signalling pathways as therapeutic targets in cancer. *Nat. Rev. Cancer* **2013**, *13*, 11−26.

(3) Lecarpentier, Y.; Schussler, O.; Hébert, J.-L.; Vallée, A. Multiple Targets of the Canonical WNT/β-Catenin Signaling in Cancers. *Front. Oncol.* **2019**, *9*, 1248.

(4) Doghman, M.; Cazareth, J.; Lalli, E. The T cell factor/beta-catenin antagonist PKF115−584 inhibits proliferation of adrenocortical carcinoma cells. *J. Clin. Endocrinol. Metab.* **2008**, *93*, 3222−3225.
(5) Dev, A.; Vachher, M.; Prasad, C. P. β-catenin inhibitors in cancer therapeutics: intricacies and way forward. *Bioengineered* **2023**, *14*, 2251696.
(6) Danieau, G.; et al. ICG-001, an Inhibitor of the β-Catenin and cAMP Response Element-Binding Protein Dependent Gene Transcription, Decreases Proliferation but Enhances Migration of Osteosarcoma Cells. *Pharm. Basel Switz.* **2021**, *14*, 421.
(7) Martins-Neves, S. R.; et al. IWR-1, a tankyrase inhibitor, attenuates Wnt/β-catenin signaling in cancer stem-like cells and inhibits in vivo the growth of a subcutaneous human osteosarcoma xenograft. *Cancer Lett.* **2018**, *414*, 1−15.
(8) Hwang, S.-Y.; et al. Direct Targeting of β-Catenin by a Small Molecule Stimulates Proteasomal Degradation and Suppresses Oncogenic Wnt/β-Catenin Signaling. *Cell Rep.* **2016**, *16*, 28−36.
(9) Stakheev, D.; Taborska, P.; Strizova, Z.; Podrazil, M.; Bartunkova, J.; Smrz, D.; et al. The WNT/β-catenin signaling inhibitor XAV939 enhances the elimination of LNCaP and PC-3 prostate cancer cells by prostate cancer patient lymphocytes in vitro. *Sci. Rep.* **2019**, *9* (1), 4761.
(10) Liao, H.; Li, X.; Zhao, L.; Wang, Y.; Wang, X.; Wu, Y.; Zhou, X.; Fu, W.; Liu, L.; Hu, H.-G.; Chen, Y.-G.; et al. A PROTAC peptide induces durable β-catenin degradation and suppresses Wnt-dependent intestinal cancer. *Cell Discovery* **2020**, *6* (1), 35.
(11) Boike, L.; Henning, N. J.; Nomura, D. K. Advances in covalent drug discovery. *Nat. Rev. Drug Discovery* **2022**, *21*, 881−898.
(12) Liu, Y.; Patricelli, M. P.; Cravatt, B. F. Activity-based protein profiling: the serine hydrolases. *Proc. Natl. Acad. Sci. U. S. A.* **1999**, *96*, 14694−14699.
(13) Backus, K. M.; et al. Proteome-wide covalent ligand discovery in native biological systems. *Nature* **2016**, *534*, 570−574.
(14) Weerapana, E.; Simon, G. M.; Cravatt, B. F. Disparate proteome reactivity profiles of carbon electrophiles. *Nat. Chem. Biol.* **2008**, *4*, 405−407.
(15) Spradlin, J. N.; Zhang, E.; Nomura, D. K. Reimagining Druggability Using Chemoproteomic Platforms. *Acc. Chem. Res.* **2021**, *54*, 1801−1813.
(16) Spradlin, J. N.; et al. Harnessing the anti-cancer natural product nimbolide for targeted protein degradation. *Nat. Chem. Biol.* **2019**, *15*, 747−755.
(17) Henning, N. J.; et al. Deubiquitinase-targeting chimeras for targeted protein stabilization. *Nat. Chem. Biol.* **2022**, *18*, 412−421.
(18) Boike, L.; Cioffi, A. G.; Majewski, F. C.; Co, J.; Henning, N. J.; Jones, M. D.; Liu, G.; McKenna, J. M.; Tallarico, J. A.; Schirle, M.; Nomura, D. K.; et al. Discovery of a Functional Covalent Ligand Targeting an Intrinsically Disordered Cysteine within MYC. *Cell Chem. Biol.* **2021**, *28*, 4−13.e17.
(19) Won, S. J. et al.Redirecting the pioneering function of FOXA1 with covalent small molecules. *BioRxiv Prepr. Serv. Biol.* 2024. .
(20) Takahashi, M. et al.DrugMap: A quantitative pan-cancer analysis of cysteine ligandability. *BioRxiv Prepr. Serv. Biol.* 2023. .
(21) Zanon, P. R. A.; Lewald, L.; Hacker, S. M. Isotopically Labeled Desthiobiotin Azide (isoDTB) Tags Enable Global Profiling of the Bacterial Cysteinome. *Angew. Chem., Int. Ed.* **2020**, *59*, 2829−2836.
(22) Weerapana, E.; et al. Quantitative reactivity profiling predicts functional cysteines in proteomes. *Nature* **2010**, *468*, 790−795.
(23) Hartung, I. V.; Rudolph, J.; Mader, M. M.; Mulder, M. P. C.; Workman, P. Expanding Chemical Probe Space: Quality Criteria for Covalent and Degrader Probes. *J. Med. Chem.* **2023**, *66*, 9297−9312.
(24) Losi, L.; Zanocco-Marani, T.; Grande, A. Cadherins down-regulation: towards a better understanding of their relevance in colorectal cancer. *Histol. Histopathol.* **2020**, *35* (12), 1391−1402.
(25) Thakur, R.; Mishra, D. P. Pharmacological modulation of beta-catenin and its applications in cancer therapy. *J. Cell. Mol. Med.* **2013**, *17*, 449−456.
(26) Parrish, M. L.; Broaddus, R. R.; Gladden, A. B. Mechanisms of mutant β-catenin in endometrial cancer progression. *Front. Oncol.* **2022**, *12*, 1009345.
(27) van der Wal, T.; van Amerongen, R. Walking the tight wire between cell adhesion and WNT signalling: a balancing act for β-catenin. *Open Biol.* **2020**, *10*, 200267.
(28) Chong, P. S. Y.; et al. Non-canonical activation of β-catenin by PRL-3 phosphatase in acute myeloid leukemia. *Oncogene* **2019**, *38*, 1508−1519.
(29) Li, J.; et al. SLC38A4 functions as a tumour suppressor in hepatocellular carcinoma through modulating Wnt/β-catenin/MYC/HMGCS2 axis. *Br. J. Cancer* **2021**, *125*, 865−876.
(30) Lei, Z.; et al. Activation of Wnt/β-catenin pathway causes insulin resistance and increases lipogenesis in HepG2 cells via regulation of endoplasmic reticulum stress. *Biochem. Biophys. Res. Commun.* **2020**, *526*, 764−771.
(31) Khalifa, O.; Al-Akl, N. S.; Errafii, K.; Arredouani, A. Exendin-4 alleviates steatosis in an in vitro cell model by lowering FABP1 and FOXA1 expression via the Wnt/-catenin signaling pathway. *Sci. Rep.* **2022**, *12*, 2226.
(32) Poncet, N.; Halley, P. A.; Lipina, C.; Gierliński, M.; Dady, A.; Singer, G. A.; Febrer, M.; Shi, Y.-B.; Yamaguchi, T. P.; Taylor, P. M.; Storey, K. G.; et al. Wnt regulates amino acid transporter Slc7a5 and so constrains the integrated stress response in mouse embryos. *EMBO Rep.* **2020**, *21* (1), No. e48469.
(33) Connelly, C. M.; Boer, R. E.; Moon, M. H.; Gareiss, P.; Schneekloth, J. S. Discovery of Inhibitors of MicroRNA-21 Processing Using Small Molecule Microarrays. *ACS Chem. Biol.* **2017**, *12*, 435−443.
(34) Winter, G. E.; et al. DRUG DEVELOPMENT. Phthalimide conjugation as a strategy for in vivo target protein degradation. *Science* **2015**, *348*, 1376−1381.
(35) Krönke, J.; et al. Lenalidomide causes selective degradation of IKZF1 and IKZF3 in multiple myeloma cells. *Science* **2014**, *343*, 301−305.
(36) Liu, Z.; et al. Proteomic Ligandability Maps of Spirocycle Acrylamide Stereoprobes Identify Covalent ERCC3 Degraders. *J. Am. Chem. Soc.* **2024**, *146*, 10393−10406.
(37) Vinogradova, E. V.; Zhang, X.; Remillard, D.; Lazar, D. C.; Suciu, R. M.; Wang, Y.; Bianco, G.; Yamashita, Y.; Crowley, V. M.; Schafroth, M. A.; Yokoyama, M.; et al. An Activity-Guided Map of Electrophile-Cysteine Interactions in Primary Human T Cells. *Cell* **2020**, *182* (4), 1009−1026.e29.

https://doi.org/10.1021/jacs.4c05174
J. Am. Chem. Soc. 2024, 146, 16856−16865